CH9700035

THE NEUTRON REFLECTOMETER AT "SINQ"

DANIEL CLEMENS
Laboratorium für Neutronenstreuung,
ETH Zürich & Paul Scherrer Institut,
CH - 5232 Villigen PSI, Switzerland

ABSTRACT

SINQ's dedicated reflectometer will be a flexible instrument in many respect. A 'white beam time of flight' as well as a 'constant wavelength' setup are possible for reflectometric experiments in a vertical scattering geometry. The phase controlled double chopper at the beginning of the instrument together with properly chosen time channels at the detector allow for the variation of the temporal resolution. Collimation slits serve to determine the angular resolution. In combination, the resolution can be tailored to the experimental needs. Additionally, one can adjust the illumination of the sample by setting the sample table and the detector to an appropriate distance. A mounting for exchangeable mirrors can be used to supply polarized neutrons by a multilayer polarizer or monochromatic neutrons by a multilayer monochromator. When it is equipped with a supermirror as a deflecting unit one can maintain a horizontal sample position which makes reflectometry on liquid samples practicable. Remanent polarizers are assigned for the changing over of the neutron polarization. A 1 T electromagnet installed on the sample manipulation table and polarization analyzers complete the polarized reflectometry setup. Alternatively, an x-y-detector and single detectors will be available. By 1997/1998 the neutron reflectometer will be operational as a users' instrument.

1. Introduction

The physics and properties in thin films and multilayers as well as the processes in and along lipid membranes cannot be understood without a deep insight into the structure and dynamics of surfaces and interfaces. In the past years, X-ray and neutron reflectometry [1.] have been established as nondestructive microscopic probes for the investigation of stratified structures and hidden interfaces. Reflectometric measurements using X-ray can be traced back to 1931 [2.]. Neutrons were introduced to the technique by the first observation of the total reflection of neutrons from a surface up to a critical angle ϑ_c by Zinn and Fermi in 1944 [3. - 5.]. In the following, the measurement of ϑ_c developed to one of the first methods to determine the scattering length b of the elements. Nevertheless, only with the advent of sophisticated deposition apparatuses and techniques to produce two dimensional and isotope labeled soft matter films, together with the development of complementary characterization methods, like SIMS, RBS, Mößbauer spectroscopy, AES, XPS, ICP, TEM, AFM, etc., the method 'boomed' not

earlier than in the last two decades. Consequently, the scheduled beam-time at neutron scattering centers providing reflectometers to a user community is heavily overbooked. The unique interaction of the neutron with matter allows in the case of this measurement technique to determine quantitatively layer thicknesses, roughness at interfaces and surfaces, interdiffusion parameters, and magnetic moments in thin films and multilayers, within the film and at the interfaces. Reflectometry can contribute to research on phenomena like growth, wetting, absorption, adhesion, (inter-)diffusion, corrosion, nanocrystalline materials, magnetism, and thin film superconductivity. Many of these are relevant for industrial applications. The contrast variation method can be exploited to enhance the signal obtained from the sample. Polarized neutrons are of excellent value for investigations of magnetic materials.

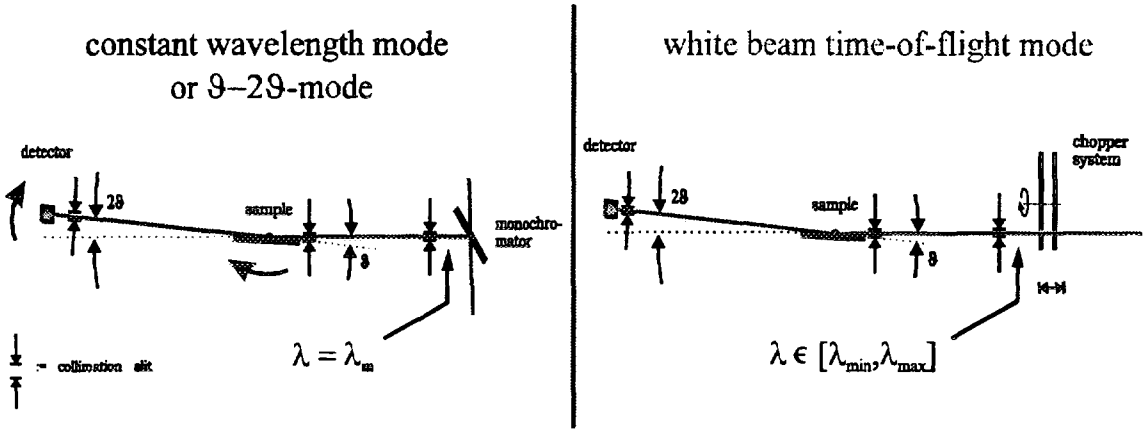

Fig. 1. Principal setup of a fixed wavelength and a white beam time-of-flight reflectometer

In principle, reflectometry can be performed using monochromatic radiation as got by reflection from a monochromator and scanning the sample in angles, i.e. for specular reflectivity, a ϑ–2ϑ–scan giving $R = R(\vartheta)$, or in the white beam time of flight (TOF) mode. In the TOF mode, the time neutrons take from a pulsed origin to the detector is measured in a fixed geometry (Fig. 1). With it one measures R as a function of time of flight which can be translated to a function of velocity $R = R(v)$ or wavelength $R = R(\lambda)$, respectively. The TOF mode is usually implemented in reflectometers at spallation sources [6. - 8.], whereas the constant wavelength (CW) mode is typical for instruments at continuous neutron sources [9.,10.].

Considering an interface between vacuum and a medium (Fig. 2) total reflection occurs because no wave field can propagate in the medium for $\vartheta < \vartheta_c$. Only an evanescent wave exists near to the boundary.

Taken

$$n = \frac{k_{med}}{k_{vac}} = \sqrt{\frac{\frac{2m}{\hbar^2}(E - V_{opt})}{\frac{2m}{\hbar^2}E}} = \sqrt{1 - \frac{V_{opt}}{E}} \cong 1 - \frac{V_{opt}}{2E} = 1 - \frac{\frac{2\pi\hbar^2}{m}\rho_{sc}}{2\frac{\hbar^2 k^2}{2m}} = 1 - \frac{\lambda^2}{2\pi}\rho_{sc} \qquad (1),$$

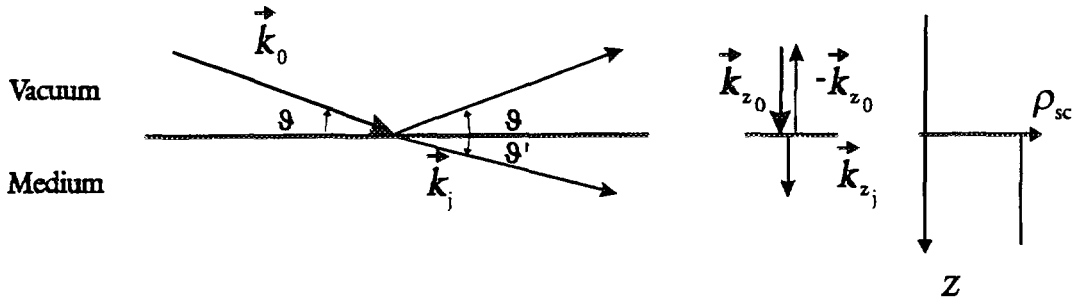

Fig. 2. Refraction of a wave at the interface to a medium j: geometry, normal components of the vectors, and scattering length density profile (from left to right)

as the refractive index, where V_{opt} is the optical potential, i.e., the average over the Fermi pseudo potential:

$$V_{opt}^{\pm}(\vec{r}) = \frac{2\pi\hbar^2}{m}\left\langle \sum_i (b_i \pm p_i)\cdot\delta(\vec{r}-\vec{r}_i)\right\rangle = \frac{2\pi\hbar^2}{m}\rho_{sc}^{\pm}(\vec{r}) \tag{2}$$

where

$$\rho_{sc}^{\pm} = \rho_{at}\cdot(b \pm p) \tag{3}$$

is the scattering length density for neutrons polarized parallel (+) or antiparallel to the quantization axis (ρ_{at} atom density, b: complex scattering length with σ_a and σ_i in the imaginary part, and p: magnetic scattering length). Herein, a Zeeman term has to be added to the purely nuclear potential if the scattering is also by the magnetic moments in the medium. This is expressed by

$$p = \frac{2m}{\hbar^2}\vec{\mu}_n\cdot\vec{B}_\perp \tag{4},$$

where $\vec{B}_\perp$ denotes the field component in the magnetic medium perpendicular to $\vec{Q}$. In reflectometry $\vec{B}_\perp$ lies in a plane parallel to the surface of the sample. And, if the polarization of the beam is realized through reflection from a magnetized mirror, the direction of $\vec{B}_{\perp,pol}$ at that polarizer determines the quantization axis for the experiment.

The optical laws also hold for the neutron wave [11.]. Taking Snell's law

$$n = k_j/k_0 = \cos\vartheta/\cos\vartheta' \tag{5}$$

at the limit where $\cos\vartheta' = 0$, with the expansion $\cos\vartheta \approx 1 - \vartheta^2/2$, and using Eq. 1, one finds an expression for the critical angle ϑ_c:

$$\vartheta_c = \lambda\sqrt{\frac{\rho_{sc}}{\pi}} \tag{6}.$$

For $\vartheta > \vartheta_c$ the wave field of the reflected beam is governed by the Fresnel equations which gives a specular reflectivity R_0 according to Porod's law:

$$R_0(Q) \propto Q^{-4} \tag{7}$$

Actually, $R(Q)$ is the Fourier transform of the scattering length density. The effect of interface roughness at a planar boundary between media i and j on $R(Q)$ can be taken into account by a static, Debye-Waller like factor in the form [12.]

$$R(Q) = R_0(Q)\, e^{-4k_{z_i}k_{z_j}\langle\sigma^2\rangle}, \quad k_{z_{i,j}} = k \sin \vartheta_{i,j} \tag{8}.$$

In the exponential of Eq. 8 σ denotes a root mean square (rms) value or the variance of a Gaussian roughness profile. The situation for multiple parallel interfaces involves refraction and (multiple) reflection at every boundary between materials with different ρ_{sc}, as well as the absorption for propagating partial waves within the layers. It can be calculated in the frame of a matrix formalism that provides one matrix for every interface. The product of these matrices describes the scattering of the whole sample and can be used to simulate the spectrum of its specular reflectivity [13. - 15.]. Roughness can be taken into account for every interface following the concepts in Ref. [16.]. Equivalently, recursion formulae can be used to calculate the theoretical reflectivity [1.]. For a spin-dependent matrix formalism see [17.]. For the analysis of the off-specular reflectivity theories on the basis of the distorted wave born approximation have been developed [18. — 21.] that give information about the in-plane structure of the interface.

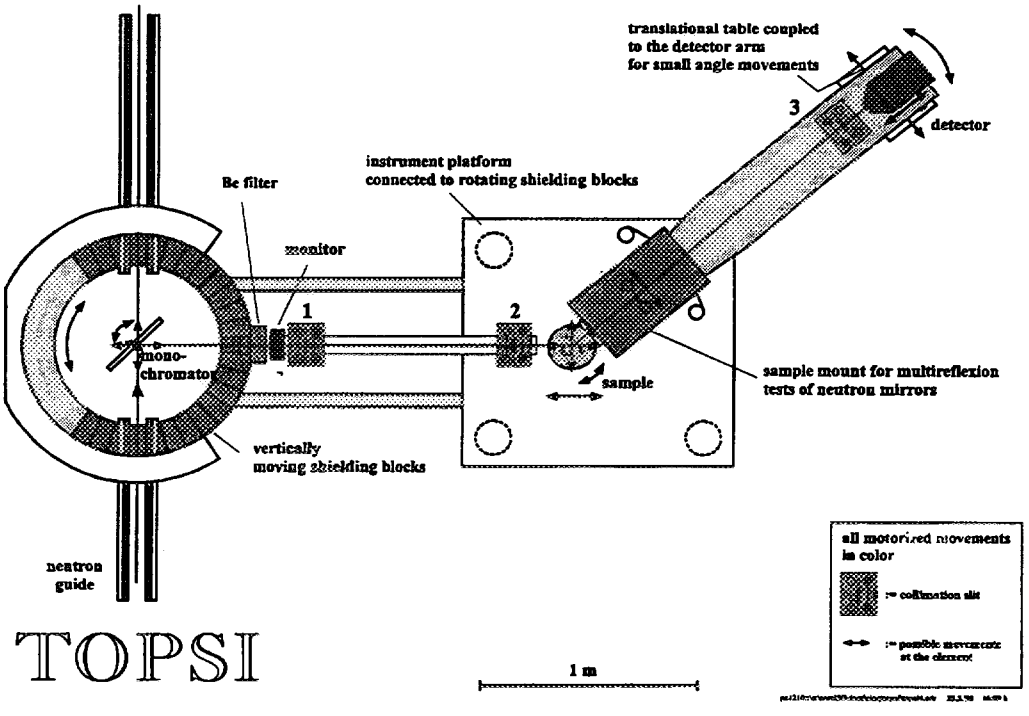

Fig. 3. Sketch of the TOPSI two axis spectrometer on a cold neutron guide

At SINQ two instruments will serve the interested user for reflectometry with neutrons. A two axis/neutron optics spectrometer (TOPSI, Fig. 3) working with cold neutrons in constant wavelength mode in a horizontal scattering geometry has been moved from the decommisioned SAPHIR reactor to the new source. At SAPHIR it has been vastly used to characterize the neutron mirrors that now build up the SINQ neutron guides. For its position at SINQ it has been extended to a multi-purpose instrument.

There are restrictions to the possible reflectometric measurements on TOPSI, especially as its partly running with other two axis experiments. Therefore, a concept for a dedicated reflectometer for SINQ has been worked out which is meant to supply users from Switzerland and abroad with a modern and precise facility, that is flexible enough to meet most of the requirements that are connected with their specific experiment.

2. Instrumental Considerations

The end position of one guide (1RNR17) is solely assigned to the neutron reflectometer which will be constructed as part of the first instrumentation program. The guide has a cross section of 50 mm * 50 mm. The supermirror coated walls reflect up to two times the critical angle of natural nickel ($\vartheta_m = m \cdot \vartheta_c(\mathrm{Ni})$, $m = 2$) with a reflectivity of 86% and more. The guide geometry leads to a nominal cut off wavelength $\lambda_c = 0.19$ nm. A ray tracing calculation which takes into account the geometry of the cold source as well as the guide [22.] shows that the cold flux (per mA proton current) at 1RNR17 will be rather high. A comparison to values measured for H15 at the I.L.L. in Grenoble is given in Fig. 5.

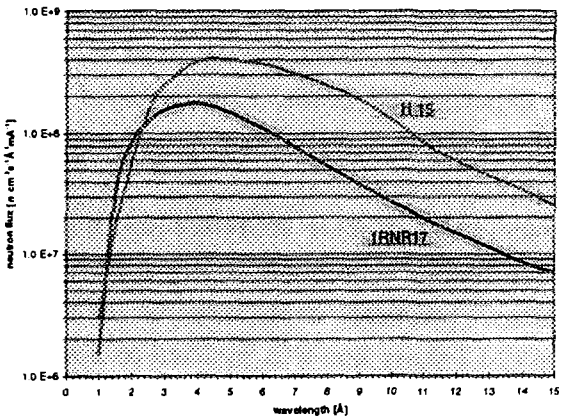

Fig. 4. Comparison of the flux at the cold neutron guides H15 (ILL) and at 1RNR17 (for a proton current of 1 mA impinging on a Pb target, calculated by P.Allenspach)

The fixed geometry in the white beam TOF mode offers advantages over the fixed wavelength mode. They are closely connected to the resolution terms. The resolution in Q for a TOF reflectometric experiment is given by

$$\frac{(\Delta Q)^2}{Q^2} = \frac{(\Delta t_{\mathrm{tch}})^2 + (\Delta t_{\mathrm{pul}})^2}{t^2} + \frac{(\Delta\vartheta)^2}{\vartheta_i^2} \qquad (9),$$

where $\Delta\vartheta$ is the geometrical resolution for the incident beam direction, Δt_{pul} is the pulse width, and Δt_{tch} is the time channel window for neutrons passing the distance L from the pulse source (spallation target or chopper) to the detector in a time t. Each of the contributions can be chosen to give almost equal values. The difference in $\Delta t_{\mathrm{pul}}/t$ for neutrons of different velocity can be balanced by adjusting the time channels

appropriately, in order to get a constant $\Delta t/t$. $\Delta\vartheta/\vartheta$ is constant, due to the fixed geometry. In the two-axis mode the resolution for specular reflection is given by

$$\frac{(\Delta Q)^2}{Q^2} = \frac{(\Delta\lambda)^2}{\lambda^2} + \frac{(\Delta\vartheta)^2}{\vartheta_i^2}. \qquad (10),$$

where $\Delta\lambda$ is dominated by the mosaicity of the monochromator, and $\Delta\vartheta/\vartheta$, again, depends on the geometry. Hence, for fixed collimation slit widths the relative angular resolution changes during the experiment, but can be held constant using programmable slits. This gives a constant 'footprint' on the sample as it is guaranteed in the TOF mode in any case. For TOF the resolution terms do not change during the scan. They are easy to match, independently. In the fixed wavelength mode the matching of the resolution terms depends on the mosaicity of the monochromator. This is coupled to the beam collimation and therefore the flexibility in the adjustment of the instrumental resolution is restricted [6.]. It is pleasing that preliminary results can be acquired in the TOF mode due to the fact that every measured burst contains information about $R(Q)$.

For a chosen resolution the instrument can be adapted to the area of interest on the sample by changing the length of the primary and secondary arm. In most cases, this is not possible for very low angles of incidence ϑ_i. TOF reflectometry usually operates at $\vartheta_i \sim 0.5°$ or higher. Therefore, and contrary to the fixed wavelength mode, its geometry is fully adaptable to the experimental needs. Predetermined by the measurement pinciple there are no or only few sample movements required except for the initial orientation. This minimizes possible positioning errors.

Despite the conveniences of TOF reflectometry, the substantial drawback of the lacking beam brightness for an instrument installed on a continuous source has to be considered. Nevertheless, practical experience at existing instruments [23.] and theoretical calculations [24.] show that it is justified to install a TOF reflectometers at a reactor.

Fig. 5 shows the principal setup of the reflectometer. To keep a high degree of flexibility the main elements are mounted on tables riding on an optical bench, where they

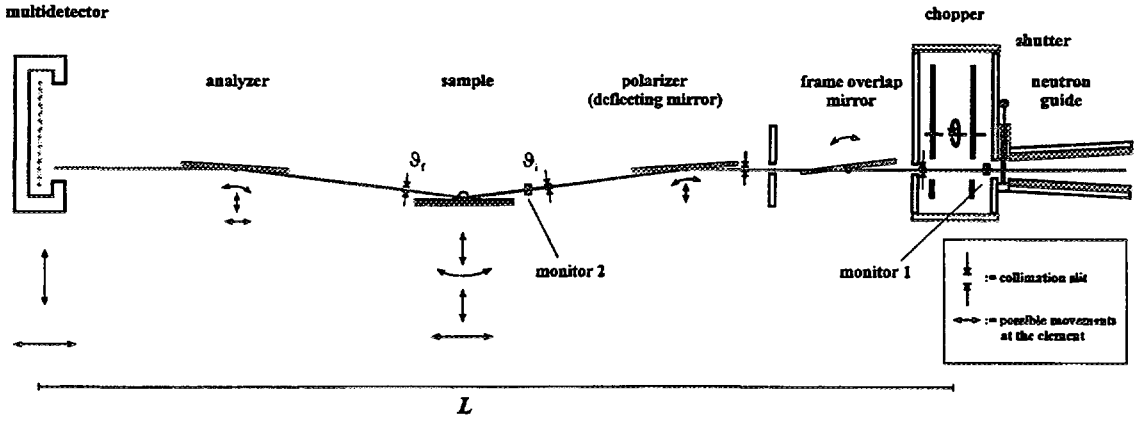

Fig. 5. Sketch of the overall instrumental layout of the propsed SINQ reflectometer. Components for the generation of magnetic fields and positioning aids are omitted.

can be moved by hand along the beam direction. The precision rotations and translations indicated for each table are made by motorized units. By the use of a deflecting mirror in this position one can achieve a horizontal sample geometry. This is an important option for measurements on liquids and can be helpful in the operation of sample environments that have a low flexibility or a large mass. Optionally, a spin analyzer can be installed on the secondary arm of the instrument for spin polarized reflectometry. In the primary arm a guidance of vertical supermirror segments reduce the losses due to the horizontal divergence of the beam.

Exceeding the requirements for a TOF reflectometer with a wide application field, the flexibility of the setup can be exploited to take advantage of the ϑ–2ϑ–mode. It is possible to move the chopper out of the beam and to replace the deflecting mirrors by a multilayer monochromator. The layer sequence of it has to be specially designed to reflect a wavelength band according to the resolution requirements. Prototype monochromators of this type have been recently produced and tested by our group. The original concept [25.] that envisaged two beam paths guided onto the same spot of the sample has been abandoned in order to simplify the mechanical layout.

3. Description of the instrument components

3.1. Chopper

On our continuous source the chopper defines the origin of a white beam neutron burst. To afford for the flexibility of the instrument one can adjust the rotation frequency

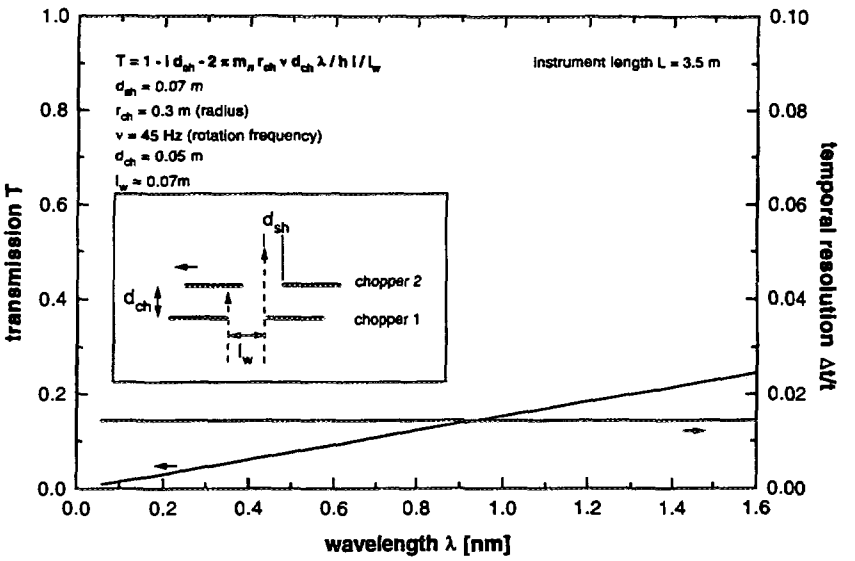

Fig. 6: Transmission function and temporal resolution, optimized for a $\Delta t_{pul}/t = 0.014$ at a constant value

ν and the width of the gating window. The frequency of the chopper has to be adapted to the length of the flight path, which can be varied in order to illuminate the sample optimally at a chosen resolution and take-off angle. Thus, to prevent a second neutron

burst from interference with the foregoing, the chopper frequency can be chosen between $\nu = 20$ Hz and $\nu = 100$ Hz. Depending on the length L of the instrument, i.e. the distance chopper to detector, and on the wanted time resolution, opening times t_{pul} of tens to hundreds of microseconds have to be realized. The width d_{sh} of the chopper window which is situated at a radius r_{ch} to the axis of the chopper disk shall be variable in the range of 1 mm to 20 mm to get an optimal adaption of $\Delta t_{pul}/t$ to the other resolution terms. A method to provide the desired variable chopper window is to rotate two identical chopper disks with an adjustable phase delay and adjustable distance d_{ch} to one another. The concept of having a constant, wavelength independent $\Delta t_{pul}/t$ has been worked out in Ref. [26.]. A corresponding setup is displayed in Fig. 6.

3.2. Frame overlap mirrors

Frame overlap mirrors are put into the primary arm in order to remove the slowest portion of the neutrons in the burst which might be reached by neutrons of the succeeding burst at the locus of the detector. Undesired neutrons with $\lambda > 1.3$ nm can easily be eliminated from the beam when they are reflected from a supermirror. The supermirrors can be coated on the two faces of a silicon wafer, so that the device transmits only 0.5% at ϑ_m. As the frame overlap mirrors shall cover a maximum beam height of 20 mm their length would exceed up to 0.5 m.

3.3.Deflecting mirrors / polarizers

An important part for the desired flexibility of the instrument is the cradle that holds the deflecting mirrors. High performance Ni-Ti-supermirrors [27.], reaching cut-off angles $\vartheta_c = m \cdot \vartheta_c(\mathrm{Ni})$ from $m = 2$ up to $m = 4$, will be used to reflect neutrons onto the sample under the chosen angle of inclination. A single segment with a total length of 1 m has to be used to accept the beam even for a relaxed angular resolution. Because the total extension L of the reflectometer can be varied and with it the sample position.

Tab. I: Characteristics of the deflection units

	deflection unit
number of segments	1
length of supermirror per segment [mm]	1'000
width of supermirror per segment [mm]	70
tilting angle of a segment	± 5°
accuracy in angle better than	0.01°
range for vertical placement [mm]	50
min. accuracy in vertical placement [mm]	0.01

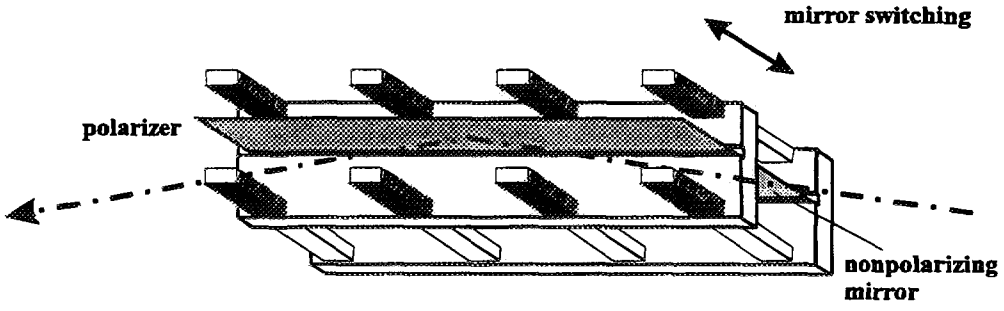

Fig. 7. Model for the principal arrangement of a polarizer and a second mirror in the deflecting unit

Parallel to a first mirror each cradle holds a second one. This can be inserted into the beam by a simple shift perpendicular to the scattering plane. With this device a deflecting mirror can be substituted by a multilayer monochromator or a polarizing mirror. Fig. 8 shows an extended reflection spectrum of a multilayer monochromator with $\Delta\lambda/\lambda = 4\%$, now in dependence of $k_z = 2\pi \sin \vartheta_i/\lambda$. The first order peak reflects neutrons with $R = 50\%$. This has been measured in a high resolution TOF mode.

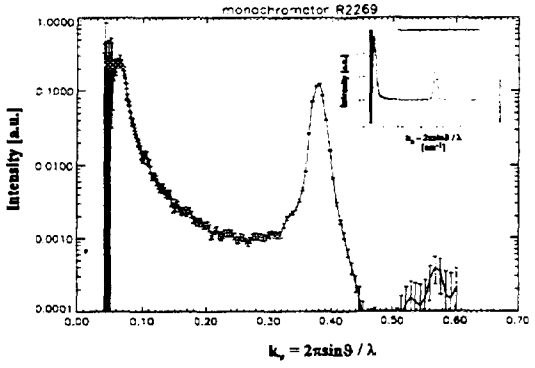

Fig. 8: Reflection from a Ni-Ti multilayer monochromator as measured in TOF mode on ROG [24.]

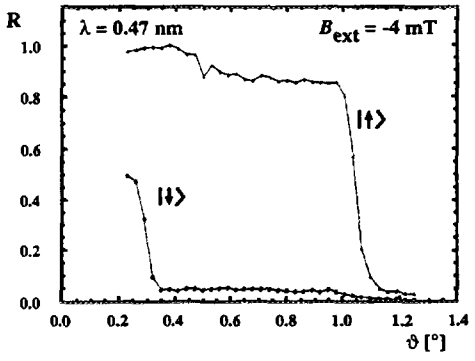

Fig. 9: Polarized neutron reflection from a 150 layer $Ti_{1-u}N_u$-$Fe_{0.50}Co_{0.48}V_{0.02}$ supermirrors in the remanent state [28.].

Polarizers consisting of a combination of $Fe_{0.50}Co_{0.48}V_{0.02}$ with Ti:N [28.] exhibit saturation in $B_{ext} \approx 20$ mT. Furthermore, their magnetization stays remanent even in small oppositely oriented magnetic fields (~5 mT). At this stage, they perform with a flipping ratio $R_{flip} \geq 40$. Consequently, there is no need for a flipper coil in the polarized neutron option. The other spin eigenstate can be reflected just by saturating the polarizer in the opposite direction and setting the field back to the value of the guide field. The needed saturation field can be provided with a simple yoke equipped with electromagnet coils. A device similar to the described deflection unit serves as a mount for an analyzer mirror.

3.4. Collimation slits

Also running on the optical benches, precision apertures are used for the angular collimation. Vertically, they shall cover a range of 0.05 mm to 20 mm with an accuracy of 0.01 mm. Each blade is directly controlled with incremental encoders. ^{6}Li is the first

choice as absorber material on the blades because it gives less contribution to the radiative background.

3.5. Sample table and sample environment

An active damping system will be placed on the positioning drives of the sample manipulation table in order to disconnect the specimen from any vibration transported through the instrument. Easy handling and exchange of the specimen can be afforded for by using special mounting plates that may be inserted onto a basis support. Proposed exchange plates are: (i) A simple flat plane with some bore-holes to fix solid samples with clamps, etc. (ii) A variable sample holder for glasses, wafers, etc., where the sample is pressed against the bottom side of a clamp. It also shall allow transmission measurements. Therefore 10 mm space has to be left open underneath the body of the sample. (iii) A plate, onto which samples can be suck by exhausting the air underneath it. Similar mounts are used in the semiconductor industry. (iv) A sample exchanger of one of these types or a combination of them. Its construction shall be made in a way, that a number of samples of a maximum size of 70 mm * 120 mm can be mounted and can be automatically brought into a position, that was previously stored as a result of the alignment procedure, and (v) a trough for the reception of liquids (70 mm * 200 mm * 5 mm). Additional sample holders and compact sample environments can be produced later according to the demands of the users. Parallel to the rotation axis of the ω-circle a maximum magnetic field of $B = 1$ T shall be applicable. Additionaly a superconducting magnet is purchased by our laboratory, reaching $B = 2$ T homogeneously over 25 mm. The alignment of the sample will be facilitated by a laser beam, fed in parallel to the neutron beam path at a position in front of the deflection mirrors. Furthermore, the tilting angle at the sample can be controlled by a precision inclinometer that the experimenter may attach to the sample holder.

3.6. Detectors

Two kinds of detectors are considered for the reflectometer. A position sensitive x-y-detector and alternatively a set of two single detectors. The single detectors serve as standard detectors for routine specular reflectometric measurements. If we can provide an analyzer mirror that divides the beam into two analyzed shares by reflecting one spin state and transmitting the other ($Fe_{0.89}Co_{0.11}$-Si-supermirror [29.]) both signals can be measured simultaneously. For neutron detection in reflectometry a low background and a high thermal neutron sensitivity, combined with a good localization of the detection event is essential. In cooperation with a research group at the ILL our lab is developing ^{3}He microstrip detectors. With its sensitive area of 172 mm * 190 mm it can cover the reflected beam under almost all measurement conditions [30.]. A comparable but smaller device on the basis of a CCD camera coupled to a neutron sensitive luminescence film is commercially available but may cause problems with the accessible dynamic range and the

readout time. The concept of the ILL/PSI x-y-detector is the ideal solution to guarantee for alignment control with neutrons, accumulating data coming from diffuse reflectivity, reasonable spacial resolution (~2 mm), spacial separation but simultaneous acquisition of signals coming from two beams, low detector costs, high detection efficiency, high signal to noise ratio, and a large dynamic range. Suitable electronics are under development at PSI.

3.7. Optical bench

As the backbone for the intended flexibility of the reflectometer and basis for a high stability of the installation this part has to fulfil certain requirements. It shall have a very accurate slide track and effectively suppress vibrations. Blocks of synthetic granite are considered to match these items. The optical bench extends to a length of ~10 m beginning at the first collimation slits.

3.8. Software

The software requirements for this instrument are somewhat different from those useful for other instruments at SINQ. For the control of the instrument and the data treatment new software must be developed or existing software from other centers (e.g., IRI Delft) may be adapted, the agreement of the authors provided.

4. Conclusion

The concept of a new SINQ reflectometer promises to provide a modern instrument flexible enough to meet the needs of a large spectrum of polarized and nonpolarized neutron reflectometry experiments. It will be available to Swiss and international users. The operation is in time-of-flight mode but it offers an option to be converted into a monochromatic beam reflectometer using thin film multilayers as monochromators. The flexibility is achieved by means of an optical bench on which the sample manipulation table, the detector, the apertures and mirrors can be set independently. Experimental requirements to resolution and sample illumination can be matched. Recent improvements in the field of polarizing mirrors and multilayers have been implemented. The spin flipper becomes superfluous due to the magnetic hysteresis of the PSI polarizer mirrors. The installation of an ILL/PSI x-y-microstrip detector promises to fit well with the needs of diffuse neutron reflectometry. Further instrumental developments at the SINQ reflectometer should preferably flow into the enlargement of available sample environments, i.e. a cryostat, a furnace, a deposition chamber for in-situ studies of growing metallic films.

Tab. II: Main characteristics of the SINQ reflectometer

neutron guide		
	cold source	D_2
	λ_{peak}	0.4 nm
	simulated peak flux	$1.8 * 10^8$ $ns^{-1}cm^{-2}mA^{-1}$, for Pb target
	coating	Ni-Ti-supermirrors, $\vartheta_c = 2\vartheta_c(Ni)$
	cross section	50 mm * 50 mm
	λ_c from simulation	0.1 nm
chopper		
	disks	2, side by side, phase coupled
	gating frequency	20 ... 100 Hz
	window	1 ... 20 mm
	relative distance d_{ch}	50 ... 350 mm
frame overlap mirrors		
	type	double side supermirror on Si wafer
	length	0.5 m
	cut off wavelength	~ 1.3 nm
deflecting mirrors / polarizers		
	1 unit (see Tab. I)	supermirrors, polarizer, monochromator
collimation slits		
	slit dimensions	(0.05 ... 20 mm) * (5 ... 55 mm)
sample manipulation table		
	rotations	2 circles (ω,χ), ±10°
	translations	2 directions
sample holder / exchanger		
	4 exchangeable plates &	1 automatic exchanger
sample environment		
	electromagnet	B_{max} = 1 T
alignment aids		
	optical	laser
	electronical	inclinometer
analyzer		
		FeCo-Si (or Ti)-supermirrors
	length	60 cm
detectors		
	^{3}He x-y-microstrip	172 mm * 190 mm
	^{3}He single detectors	2, "squashed" type
maximum sample size		150 mm * 500 mm
resolution		1.5% ... 10%
total length chopper - detector	L	2.5 ... 10 m

5. References

1. See for example T.P. Russell, *Materials Science Reports* **5** (1990) 171
2. H. Kiessig, *Ann. Phys.* **10** (1931) 769
3. E. Fermi, *Collected Papers*, ed. E.Segrè (Unversity of Chicago Press, 1962), Paper no. 217
4. E. Fermi and W.H. Zinn, *Phys. Rev.* **70** (1946) 103
5. E. Fermi and W.H. Zinn, Cambridge Conference 1947, in ref. [3], Paper No. 220
6. G.P. Felcher, R.O. Hilleke, R.K. Crawford, J. Haumann, R. Kleb, and G. Ostrowski, *Rev. Sci. Instrum.* **58** (1987) 609
7. J. Penfold, R.C. Ward, and W.G. Williams, *J. Phys.* **E 20** (1987) 1411
8. A. Karim, B.H. Arendt, R. Goyette, Y.Y. Huang, R. Kleb, and G.P. Felcher, *Physica* **B 173** (1991) 17
9. M. Stamm, S. Hüttenbach, and G. Reiter, *Physica* **B 173** (1991) 11
10. H. Toews, *Ph.D. Thesis* (German), Techn. Univ. Berlin (1993); T. Robertson (ed.): *HMI Report* (BENSC) HMI-B 493, Hahn-Meitner-Institut Berlin (1993)
11. A.G. Klein and S.A. Werner, *Rep .Prog. Phys.* **46** (1983) 259
12. L. Névot and P. Croce, *J. Appl. Cryst.* **7** (1974) 125
13. J. Schelten and K. Mika, *Nucl. Instrum. Meth.* **160** (1979) 287
14. O. Schärpf, *Physica* **B 156 & 157** (1989) 631; **174** (1991) 514
15. D. Clemens, *Ph.D. Thesis* (German), Techn. Univ. Berlin (1993)
16. T. Megademini and B. Pardo, *J. Optics* **16** (1985) 289
17. G.P. Felcher, R.O. Hilleke, R.K. Crawford, J. Haumann, R. Kleb, and G. Ostrowski, *Rev. Sci. Instrum.* **58** (1987) 609
18. S.K. Sinha, E.B. Sirota, S. Garoff and H.B. Stanley, *Phys Rev.* **B 38** (1988) 2297
19. R. Pynn, *Phys Rev.* **B 45** (1992) 602
20. V. Holý, J. Kubena, I. Ohlídal, K. Lischka and W. Plotz, *Phys Rev.* **B 47** (1993) 15896
21. V. Holý and T. Baumbach, *Phys Rev.* **B 49** (1994) 10668
22. P. Allenspach, Labor für Neutronenstreuung ETH Zürich & Paul Scherrer Institut, CH-5232 Villigen PSI
23. C. Fermon, *ILL Reflectometry Workshop*, oral presentation, Grenoble (1995)
24. V.O. de Haan, *Ph.D. Thesis*, Techn. Univ. Delft (1995), ISBN 90-73861-23-3
25. D. Clemens, *Physica* **B 221** (1996) 507
26. A.A. van Well, *Physica* **B 180 & 181** (1992) 959
27. P. Böni, D. Clemens, H.P. Friedli, H. Grimmer and H. Van Swygenhoven, *Lab. für Neutronenstreuung Annual Progress Report* LNS-175 (1994)
28. D. Clemens, P. Böni, H.P. Friedli, R. Göttel, C. Fermon, H. Grimmer, H. Van Swygenhoven, J. Archer, F. Klose, Th. Krist, F. Mezei, P. Thomas, and H. Toews, *Physica* **B 213 & 214** (1995) 942
29. T. Krist, C. Pappas, T. Keller, and F. Mezei, *Physica* **B 213 & 214** (1995) 939
30. J. Schefer, P. Geltenbort, A. Oed, M. Koch, A. Isacson, N. Schlumpf and R. Thut; *Proc. Int. Workshop on Microstrip Detectors*, Legnaro, Italy, (1994)